electronics

MDPI

Article

Evaluating Multimodal Physiological Signals for Biometric Human Recognition Using GSR, ECG, and PPG Signals

Shaimaa Hagras [1,*], Hany S. Khalifa [2] and O. G. Elbarbary [1]

[1] Information Systems Department, Faculty of Computers and Informatics, Tanta University, Tanta 31733, Egypt
[2] Department of Computer Science, Misr Higher Institute of Commerce and Computers, Mansoura 35511, Egypt
* Correspondence: shaimaa_hagras@ics.tanta.edu.eg

Abstract

In recent years, physiological signal-based biometrics has gained increasing attention due to its resistance to spoofing attacks, suitability for continuous authentication, and compatibility with wearable devices. This study investigates a multimodal biometric framework based on three physiological signals: galvanic skin response (GSR), electrocardiogram (ECG), and photoplethysmography (PPG). Although GSR has demonstrated promising performance in emotion recognition and animal recognition studies, it remains relatively underexplored in biometric human recognition applications compared with ECG and PPG. As a non-invasive signal that can be easily acquired through simple skin contact, GSR offers several advantages, including low-cost sensing, ease of integration into wearable devices, user convenience, and suitability for continuous monitoring. To address this gap, the proposed framework combines features extracted from ECG, PPG, and GSR signals and employs machine learning algorithms for human recognition. The approach was evaluated using two publicly available datasets, CLAS and MAUS. Experimental results demonstrate that multimodal fusion significantly enhances recognition performance, achieving accuracies of 97% and 99% on the CLAS and MAUS datasets, respectively, with the K-Nearest Neighbors (KNN) classifier. These findings highlight the potential of integrating GSR with ECG and PPG signals to develop biometric systems for wearable and continuous authentication applications.

Keywords: biometrics; electrocardiogram (ECG); galvanic skin response (GSR); human recognition; photoplethysmography (PPG); physiological signals

Check for updates

Academic Editor: Shing-Hong Liu

Received: 6 June 2026
Revised: 20 June 2026
Accepted: 6 July 2026
Published: 7 July 2026

Copyright: © 2026 by the authors. Licensee MDPI, Basel, Switzerland. This article is an open access article distributed under the terms and conditions of the Creative Commons Attribution (CC BY) license.

1. Introduction

Human recognition using physiological signals in wearable devices is increasingly important because it offers a secure and continuous method for verifying a user's identity. Unlike traditional authentication methods, such as passwords and personal identification numbers (PINs), signal-based recognition relies on unique biological patterns, such as EEG, ECG, PPG, or GSR, which are difficult to imitate or steal. This makes wearable systems more resilient to spoofing while providing seamless real-time authentication. As wearables become more integrated into daily life for health monitoring, payments, and personalized services, reliable signal-based human recognition enhances user safety, maintains privacy, and supports more intuitive interactions with technology.

Through extensive research, the authors found that Galvanic Skin Response (GSR), also known as Electrodermal Activity (EDA), is commonly used for human emotion

recognition [1–5]. However, its application in human recognition systems remains relatively rare [6–8]. The growing ability to embed sensors into wearable devices, such as smart glasses, wristbands, and chest bands, has motivated this study. Accordingly, we evaluated the feasibility of using distinctive GSR features fused with electrocardiogram (ECG) and photoplethysmography (PPG) signals for subject recognition in a multimodal biometric system.

The GSR measures subtle changes in the electrical conductivity of the skin in response to external or internal stimuli [9]. This responsiveness to real-world conditions makes it a promising addition to human recognition models, particularly in dynamic environments where users naturally interact with stimuli.

ECG has recently been validated as a robust biometric modality. As demonstrated by prior studies, ECG signals are highly secure and reliable; they can only be captured from living individuals. Unlike electroencephalogram (EEG) signals, which may raise privacy concerns due to potential implications such as mind reading, ECG data are generally more acceptable to users. Furthermore, ECG has been explored for animal identification, like canine recognition systems [10].

PPG signals measure variations in blood volume within the vascular system and offer the significant advantage of being readily acquired through a wide range of wearable devices, such as smart watches [11]. This accessibility makes PPG particularly suitable for Internet of Things (IoT)-based applications. Although PPG-based biometric identification has been extensively studied [12,13], the majority of existing research has been conducted in controlled clinical settings involving stationary subjects, thereby limiting the influence of motion artifacts (MAs) on signal quality [14]. In contrast, the present study evaluates biometric recognition performance using datasets collected from participants engaged in diverse activities and exposed to various stimuli. Consequently, the experimental conditions more closely resemble real-world scenarios, providing a more realistic assessment of the robustness and practical applicability of PPG-based biometric systems.

This study makes three primary contributions. First, it introduces a multimodal biometric recognition framework that integrates galvanic skin response (GSR), electrocardiogram (ECG), and photoplethysmography (PPG) signals within a unified machine learning framework, specifically designed to operate under dynamic and realistic conditions. Second, it systematically investigates the effectiveness of multimodal fusion in enhancing recognition performance relative to unimodal approaches across varying levels of motion artifacts and environmental disturbances. Third, it provides empirical evidence regarding the reliability of individual physiological signals and the complementary information they contribute when combined, thereby offering practical insights for the design and deployment of wearable biometric systems.

This study is based on two key hypotheses. First, combining multiple physiological signals through multimodal fusion results in significantly improved biometric recognition performance compared with unimodal approaches. Second, incorporating galvanic skin response (GSR) signals into wearable biometric systems provides complementary information that enhances recognition accuracy and increases the suitability of such systems for real-world deployment.

2. Related Work

Many studies have focused on physiology-based biometrics with the increasing adoption of wearable and inertial sensors.

Piciucco et al. [6] investigated human recognition using signals collected via wristbands. The study involved 17 participants performing natural activities in two sessions separated by approximately seven days. Electrodermal activity and blood volume pulse

signals were fused using a CNN applied to spectrogram representations, achieving an average correct recognition rate of 98.58%.

Bianco and Napoletano [7] explored a multimodal system using four physiological signals: heart rate, breathing rate, palm electrodermal activity, and perinasal perspiration signals. They employed a one-dimensional convolutional neural network (1D-CNN) optimized using a sequential model-based optimization. Testing on 37 subjects using a public dataset in a driving simulator environment, the model achieved 99.51% accuracy with a single modality and 99.69% using a multimodal approach.

Blasco and Peris-Lopez [8] utilized low-cost wearable sensors, including ECG, PPG, GSR, and accelerometers, to develop a prototype for biometric verification. They collected data from 25 subjects performing various activities and evaluated the performance of the individuals and fused the signals. Their results demonstrated that smartwatches and fitness bands can effectively enable biometric verification, with the best performance achieved through the fusion of ECG, PPG, and GSR, resulting in a 0.02 Equal Error Rate (EER).

Yi et al. [15] proposed a feature fusion network for ECG-based recognition. Their model used an adaptive attention mechanism to emphasize the heartbeat features and reduce intersession variability. When tested on four databases, the model achieved identification accuracies of 96.31%, 73.79%, 77.80%, and 54.78%, respectively.

To enhance ECG and PPG biometric performance, Labati et al. [12] applied preprocessing, normalization, and a two-dimensional Siamese CNN (MultiCardioNet) to compare the spectrogram representations. They reported EERs of 2.15% (ECG-ECG), 2.42% (PPG-PPG), and 4.76% (ECG-PPG/PPG-ECG).

These studies collectively demonstrate the potential of physiological signals and machine learning models for human recognition classification. However, few studies have explored the GSR signal.

3. Proposed Multimodal

This section presents the proposed multimodal framework for human recognition using ECG, PPG, and GSR signals. Figure 1 illustrates the overall architecture of the proposed system. The framework consists of five main stages: signal preprocessing, segmentation, feature extraction, feature fusion, and classification. Each stage is described in detail in the following subsections.

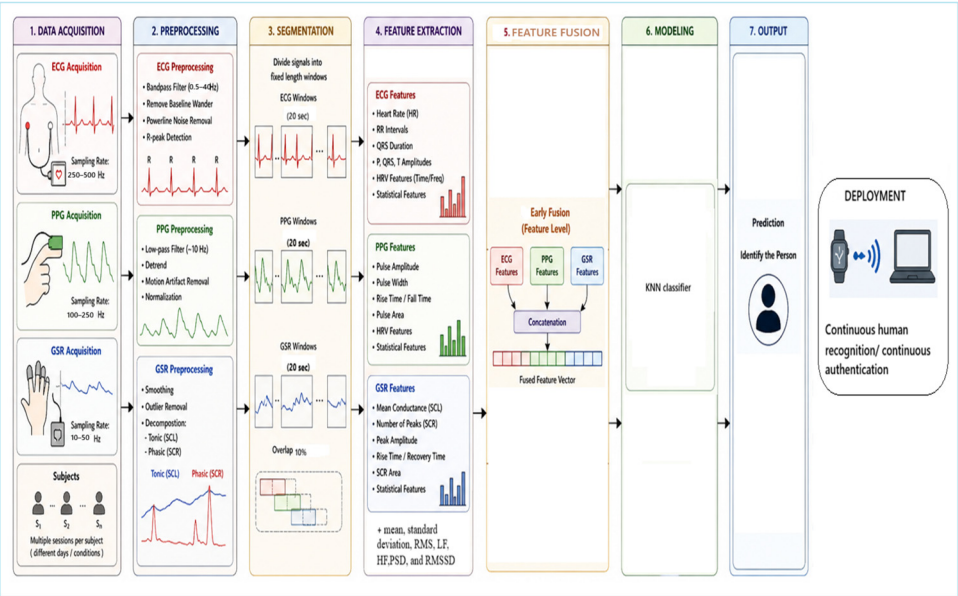


Figure 1. Proposed Multimodal framework.

3.1. Preprocessing

With significant advances in intelligent sensor technology, it has become feasible to collect high-quality physiological signals from users under various conditions, thereby enabling the development of robust recognition models and multimodal systems. In the proposed approach, raw physiological signals acquired from multiple sensors were subjected to modality-specific preprocessing techniques to improve the signal quality and enhance feature extraction. For the ECG signal, preprocessing included band-pass filtering in the range of 0.5–40 Hz, baseline wander correction, power line noise removal, and R-peak detection. The PPG signal was processed using a low-pass filter with a cutoff frequency of 10 Hz, followed by motion artifact removal and normalization. For the GSR signal, preprocessing involved signal smoothing, outlier removal, and decomposition into tonic Skin Conductance Level (SCL) and phasic Skin Conductance Response (SCR) components.

3.2. Segmentation

Following preprocessing, the physiological signals were segmented into fixed-length windows for feature extraction and classification. Several combinations of window lengths and overlap ratios were evaluated to determine the optimal segmentation strategy. Based on experimental analysis, a window length of 20 s with a 10% overlap provided the best recognition performance and was therefore adopted throughout the study. Figure 2 illustrates the recognition performance achieved under different segmentation configurations.

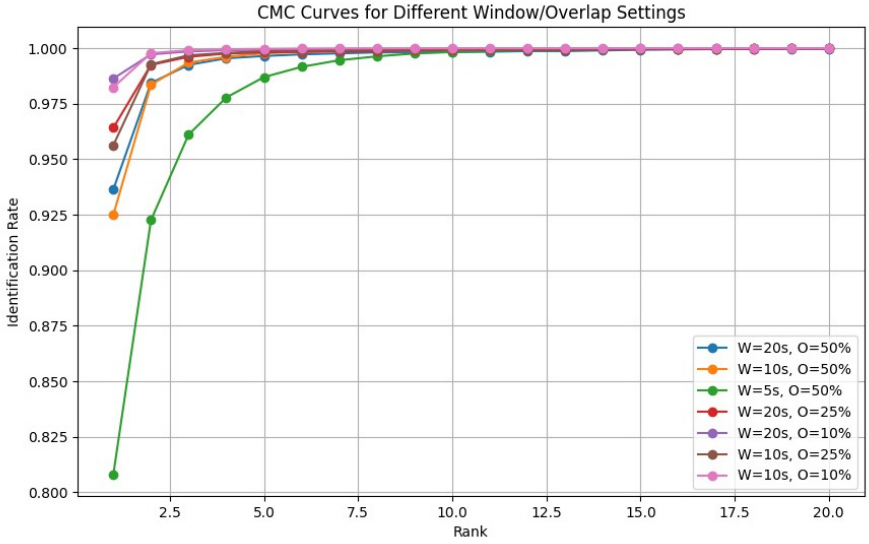


Figure 2. Comparison of the impact of different windows sizes and overlapping ratios.

3.3. Feature Extraction

A set of statistical features used in many studies [16,17] was extracted from all physiological signals, in addition to modality-specific features designed to capture the unique characteristics of each signal type. The common statistical features included mean, standard deviation, root mean square (RMS), low-frequency power (LF), high-frequency power (HF), power spectral density (PSD), and root mean square of the successive differences (RMSSD).

Mean:

$$\mu = \frac{1}{N}\sum_{i=1}^{N} X_i \quad (1)$$

where μ = mean, X_i = individual data points, and N = the number of data points.

Standard Deviation:

$$\sigma = \frac{1}{N}\sum_{i=1}^{N} (X_i - \mu_{ECG})^2 \quad (2)$$

where σ is the standard deviation, μ the mean, X_i = individual data points, and N the number of data points.

Root mean square:

$$RMS = \sqrt{\frac{1}{N}\sum_{i=1}^{N} X_i^2} \quad (3)$$

where X_i = individual data points, and N number of data points.

Low-frequency power (LF) using Power Spectral Density

$$LF = \int_{f1}^{f2} PSD(f)df \quad (4)$$

High-frequency power (HF) using Power Spectral Density

$$HF = \int_{f1}^{f2} PSD(f)df \quad (5)$$

where

LF: power within a specific low-frequency range of a signal (0.04 and 0.15)
HF: power in a higher frequency band (0.15 and 0.4)

The power spectral density (PSD) represents the distribution of the signal frequency. It is computed according to Equation (6) [18].

$$PSD(k) = \frac{2di}{n^2}((Y_{real}(k))^2 + (Y_{imag}(k))^2) \quad (6)$$

Root mean square of the successive differences (RMSSD) [19]

$$RMSSD = \sqrt{\frac{1}{N-1}\sum_{i=1}^{N-1} (RR_{interval}(i+1) - RR_{interval}(i))^2} \quad (7)$$

For the ECG signal, unique characteristics were identified (Figure 3): heart rate, RR interval, duration of the QRS complex, and amplitude of the R-peak. These attributes were chosen because of their proficiency in depicting the temporal and morphological characteristics of cardiac signals for tasks related to biometric identification and classification, as mentioned in many studies [19,20].

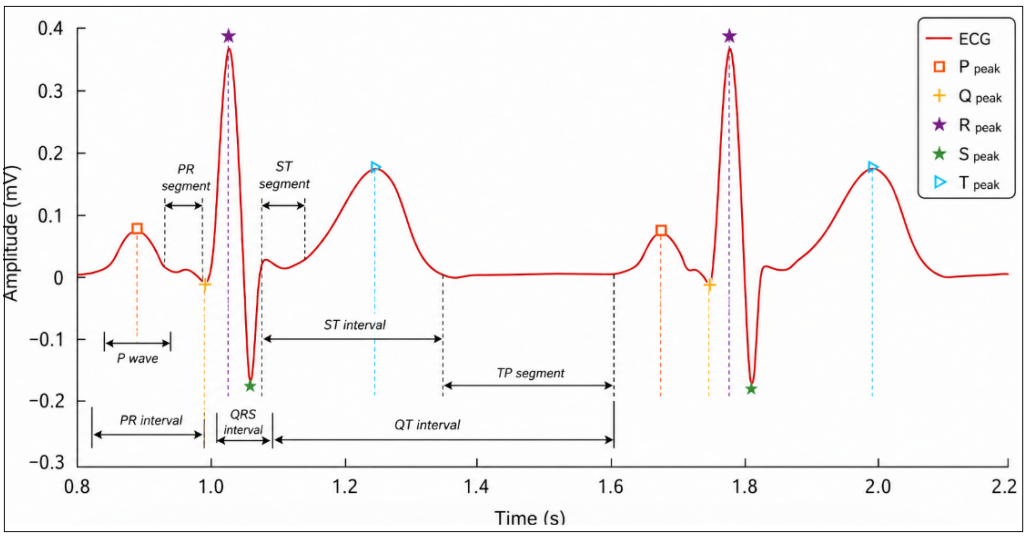


Figure 3. ECG Features.

Temporal and morphological features were extracted from the PPG signal to capture the distinct cardiovascular traits of each individual [21,22]. The obtained features include Pulse Amplitude, indicating variations in blood volume; Pulse Width, signifying the length of each pulse wave; rise and fall times, illustrating the upward and downward traits of the waveform; and Pulse Area, which quantifies the total energy distribution throughout the pulse cycle.

Multiple features were obtained from the GSR signal [23,24] to define the electrodermal activity patterns of individuals. The features obtained consist of the Mean Skin Conductance Level (SCL), which reflects the underlying conductivity of the skin over an extended period, and the Number of Skin Conductance Responses (SCR peaks), which shows the rate of swift physiological reactions. Additional morphological characteristics, such as Peak Amplitude, Rise Time, and Recovery Time, were calculated to outline the intensity and temporal dynamics of each SCR event. Additionally, the SCR Area was computed to measure the overall response energy linked to sympathetic nervous system function.

3.4. Feature Fusion

Feature-level fusion was performed by concatenating the feature vectors extracted from the ECG, PPG, and GSR signals into a single high-dimensional representation. This strategy enables the integration of complementary physiological information from multiple modalities while retaining the discriminative characteristics of each signal. The resulting fused feature vector was then used as input to the classification models for human recognition.

3.5. Model Training

During the model training phase, numerous experiments were conducted using different machine learning classifiers to evaluate the performance of the proposed biometric-recognition system. The features extracted from the ECG, PPG, and GSR signals were used to train and test several classification models, including traditional machine learning algorithms such as multilayer perceptron [25], logistic regression [26], support vector machine (SVM) [27], random forest (RF) [28], K-Nearest Neighbors (KNN) [29], and decision tree (DT) [30]. The experiments aimed to compare the classification accuracy, precision, recall, and F1-score of each model in identifying individuals based on multimodal physiological signals.

To ensure a robust and unbiased evaluation of the proposed multimodal framework, subject-wise 10-fold cross-validation was utilized, where data from each subject were kept exclusively within a single fold to prevent data leakage and reduce overfitting.

4. Experiments

The proposed multimodal framework was implemented in Python v3.11 and executed on a Windows 11 Pro (v22H2, 64-bit) operating system equipped with a 12th Gen Intel(R) Core(TM) i7-12700 processor and 16.0 GB of RAM.

We used two public datasets, CLAS [31] and MAUS [32], for this study. These datasets present several challenges. First, the participants were healthy individuals, unlike in prior studies that primarily relied on clinical data. Second, the physiological signals were recorded while the participants engaged in both cognitive and physical tasks using audio-video stimuli to simulate real-life scenarios, further enhancing the relevance of the data. All recordings were captured using wearable devices.

The CLAS dataset comprises synchronized recordings of physiological signals, including ECG, PPG, GSR, and accelerometer data. Sixty subjects were included in this study. Recordings captured each participant performing three reactive tasks and two conscious tasks, with the reactive tasks incorporating visual and audio-video stimuli. Most were students in their twenties, with one participant in their thirties, one woman in her late forties, and one subject aged 50 years. The signals were collected using wearable sensors at a sampling rate of 256 Hz and a 16-bit resolution. Each recording session lasted for approximately 30 min.

The MAUS dataset included 22 participants (two females) with an average age of 23 years. Participants performed an N-back task, a cognitive workload assessment involving varying difficulty levels, to simulate different mental load conditions. Each session lasted 35 min.

Before training the classifiers, we labeled every subject's file with a unique number (for MAUS, the labels were from 1 to 22, and for CLAS, the labels were from 1 to 60).

5. Results

To determine the best window size and overlap percentage, multiple experiments were conducted on the MAUS dataset. The comparison results indicated that the best performance was achieved using a 20 s window size with 10% overlap, which was applied in this study.

Performance was measured using many standard classification metrics: accuracy, precision, recall, F1-score, True Negative Rate (TNR), False Positive Rate (FPR), False Negative Rate) FNR, and EER. These were calculated as follows:

$$Recall = TP/(\mathrm{TP} + \mathrm{FN}) \tag{8}$$

$$Precision = TP/(\mathrm{TP} + \mathrm{FP}) \tag{9}$$

$$F1_score = 2 \times (Precision \times \mathrm{Recall})/(Precision + \mathrm{Recall}) \tag{10}$$

$$Accuracy = (TP + TN)/(\mathrm{TP} + \mathrm{TN} + \mathrm{FP} + \mathrm{FN}) \tag{11}$$

Many classifiers, including multilayer perceptron, logistic regression, decision tree, support vector machine, KNN, and random forest, were evaluated on the proposed multimodal model, with their performance summarized in Table 1 for the CLAS dataset and Tables 2–5 for the MAUS dataset. To display the results more intuitively, Figures 4 and 5 show a comparison of the recognition results of the different algorithms.

Table 1. Results of machine learning classifiers on CLAS dataset.

	ECG				**GSR-PPG**				**ECG-GSR-PPG**			
	Acc.	**Prec.**	**Rec.**	**F1.**	**Acc.**	**Prec.**	**Rec.**	**F1.**	**Acc.**	**Prec.**	**Rec.**	**F1.**
RF	0.70	0.70	0.70	0.69	0.24	0.24	0.24	0.23	0.86	0.86	0.86	0.86
Multilayer perceptron	0.74	0.74	0.74	0.73	0.18	0.17	0.18	0.14	0.87	0.87	0.87	0.87
Logistic regression	0.39	0.35	0.39	0.34	0.08	0.07	0.08	0.06	0.51	0.50	0.51	0.46
Decision Tree	0.83	0.83	0.83	0.83	0.22	0.22	0.22	0.22	0.94	0.94	0.94	0.94
SVM	0.43	0.41	0.43	0.39	0.08	0.09	0.08	0.06	0.56	0.57	0.56	0.53
KNN	0.88	0.88	0.88	0.87	0.24	0.25	0.24	0.24	0.97	0.97	0.97	0.97

Table 2. Accuracy of machine learning classifiers on MAUS dataset.

	Accuracy					
	ECG	**PPG**	**GSR**	**GSR-ECG**	**GSR-PPG**	**ECG-GSR-PPG**
RF	0.77	0.74	0.71	0.90	0.78	0.98
Multilayer perceptron	0.89	0.72	0.78	0.93	0.79	0.97
Logistic regression	0.86	0.72	0.74	0.93	0.75	0.97
Decision Tree	0.91	0.75	0.74	0.93	0.78	0.98
SVM	0.89	0.77	0.75	0.92	0.77	0.98
KNN	0.93	0.78	0.71	0.94	0.78	0.99

Table 3. Precision of machine learning classifiers on MAUS dataset.

	Precision					
	ECG	**PPG**	**GSR**	**GSR-ECG**	**GSR-PPG**	**ECG-GSR-PPG**
RF	0.77	0.74	0.71	0.91	0.78	0.98
Multilayer perceptron	0.89	0.72	0.78	0.93	0.79	0.97
Logistic regression	0.86	0.72	0.74	0.92	0.75	0.97
Decision Tree	0.91	0.75	0.74	0.93	0.78	0.98
SVM	0.88	0.77	0.75	0.92	0.77	0.98
KNN	0.93	0.78	0.71	0.94	0.77	0.99

Table 4. Recall of machine learning classifiers on MAUS dataset.

	Recall					
	ECG	**PPG**	**GSR**	**GSR-ECG**	**GSR-PPG**	**ECG-GSR-PPG**
RF	0.77	0.74	0.71	0.90	0.78	0.98
Multilayer perceptron	0.89	0.72	0.77	0.93	0.79	0.97
Logistic regression	0.86	0.72	0.74	0.93	0.74	0.97
Decision Tree	0.91	0.75	0.74	0.93	0.78	0.98
SVM	0.89	0.76	0.75	0.92	0.77	0.98
KNN	0.93	0.78	0.71	0.94	0.78	0.99

Table 5. F1-score of machine learning classifiers on MAUS dataset.

	F1-Score					
	ECG	**PPG**	**GSR**	**GSR-ECG**	**GSR-PPG**	**ECG-GSR-PPG**
RF	0.77	0.74	0.71	0.90	0.78	0.98
Multilayer perceptron	0.88	0.72	0.78	0.93	0.79	0.97
Logistic regression	0.86	0.72	0.73	0.93	0.75	0.96
Decision Tree	0.91	0.75	0.74	0.93	0.78	0.98
SVM	0.89	0.77	0.75	0.91	0.77	0.97
KNN	0.93	0.78	0.71	0.94	0.78	0.99

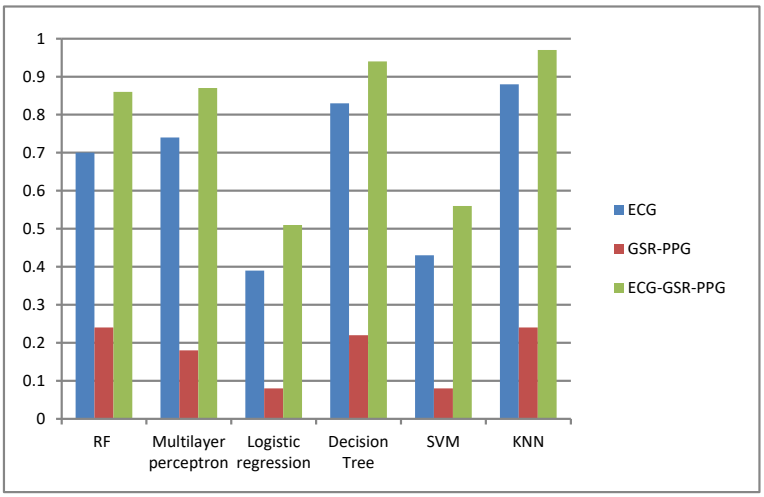


Figure 4. Accuracy of six machine learning algorithms on CLAS dataset.

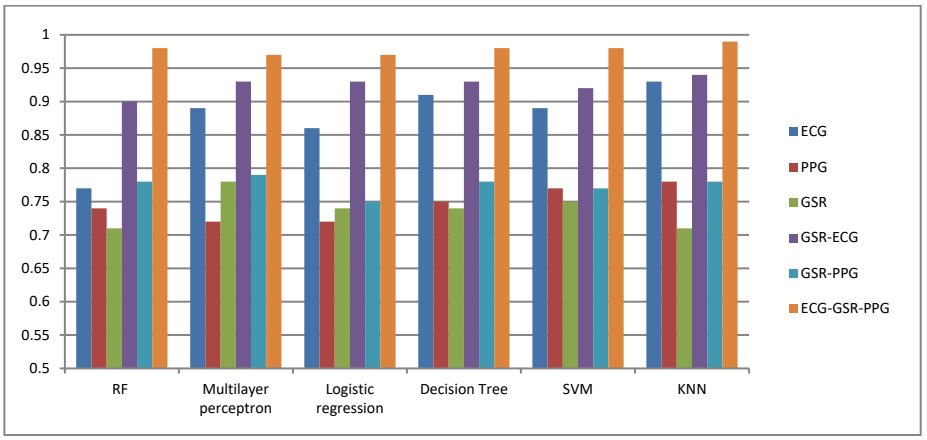


Figure 5. Accuracy of six machine learning algorithms on MAUS dataset.

The Equal Error Rate (EER) was also employed to evaluate the biometric performance of the proposed system. The EER was computed using the distance scores generated by the KNN classifier. The EER was evaluated using a verification framework. Specifically, the Euclidean distance was computed between each test sample and the enrolled template. Distances corresponding to the true identity were treated as genuine scores, whereas those corresponding to all other identities were treated as impostor scores. By varying the decision threshold across the range of Euclidean distance scores, the False Acceptance Rate (FAR) and False Rejection Rate (FRR) were calculated. The EER was then determined at the threshold where the FAR and FRR were equal. The proposed multimodal model demonstrated strong performance across both datasets, achieving an Equal Error Rate (EER) of 0.72% on the CLAS dataset and an EER of 0.4% on the MAUS dataset. These results indicate a high level of discriminative capability and robustness of the proposed model.

Based on a comprehensive literature search and the overall performance reported in Table 6, it is clear that the use of GSR signals in biometric research remains limited; only three studies [6–8] have incorporated GSR primarily within multimodal frameworks that achieve high recognition accuracy. These findings highlight the need for further investigation and broader experiments on additional datasets to better demonstrate the potential of GSR in reliable human recognition. Furthermore, the proposed multimodal framework demonstrated good performance compared with the state-of-the-art methods reported in the literature.

Table 6. The proposed multimodal framework compared with literature models.

Paper	Data Set	Size	Signal	Classifier	Accuracy %
[6]	based on their custom dataset	17	Fusion of EDA and BVP	CNN	98.58
[7]	by Taamneh et al.	37	Fusion of HR, BR, P-EDA, and PER-EDA	1D-CNN	99.69
[8]	based on their custom dataset	25	Fusion of ECG, PPG and GSR	Gaussian model	99
[12]	CapnoBase PRRB	42	ECG-ECG, PPG-PPG, Fusion of ECG and PPG	MultiCardioNet, a Siamese CNN	EER 2.15 EER 2.42 EER 4.76 Respectively
[13]	PhysioNet	50 12	ECG PPG	CNN CNN	94 90
[15]	ECG-ID, PTB Diagnostic ECG, CYBHi, Heartprint	90 290 65 199	ECG	domain adaptive technology	96.31, 73.79, 77.80, 54.78 Respectively
[33]	BIDMC	53	PPG	MSF-SE ResNet50	98.41
[34]	based on their custom dataset	40 27	Fusion of PPG and fingerprints	homogeneous neural network	100 94.3 Respectively
[35]	CapnoBase, Bidmc, BioSec2	43 53 100	PPG	one-class classification algorithms, LOF, OCSVM, EE, and IF	93.5 91.8, 95
[36]	based on their custom dataset	12	PPG	RF	62.8
[37]	P6ms MAUS	12 22	PPG	SVM	>90 for two datasets
[24]	CU-ECG MIT-BIH ECG	95 48	ECG	SVM	93 98.5 Respectively
[38]	based on their custom dataset	199	fingerprint, iris, and ECG	A convolutional Swin Transformer	99
[39]	based on their custom dataset	31	Fusion of ECG and PPG	fiducial technique with statistical properties	99.17
[40]	based on their custom dataset	22	Fusion of ECG and PPG	SVM	93.86
[41]	based on their custom dataset	45	ECG and IRIS	Decision tree	96.55
[42]	CEBS	20	ECG, SCG, and PPG	intelligent cosine similarity-based authentication module	99.79
[43]	HSCT-11	40	PCG	DNN	85.87
[44]	self-collected	32	ECG and PCG	Linear discriminant classifier as well as ensemble subspace discriminant	100
[45]	based on their custom dataset	20	EEG	CNN	95.34
ours	**CLAS** **MAUS**	**60** **22**	**Fusion of ECG, GSR and PPG**	**KNN**	**97** **99** **Respectively**

The obtained results demonstrate the effectiveness of the proposed multimodal approach for human recognition under varying cognitive and mental workload conditions. In the CLAS dataset, participants performed both reactive and conscious tasks, with the reactive tasks involving visual and audio-visual stimuli. In contrast, the MAUS dataset employed an N-back task with multiple difficulty levels to induce different levels of cognitive workload. The differences observed between the two datasets may be attributed to several factors, including variations in sensor devices, the number of participants, the nature of the performed tasks, and the types of stimuli used during data acquisition.

Despite these differences, the proposed multimodal framework consistently achieved strong recognition performance across both datasets, indicating the effectiveness of integrating GSR with ECG and PPG signals for biometric recognition. The results suggest that GSR provides complementary physiological information that can enhance recognition accuracy when combined with other physiological modalities. Nevertheless, the use of GSR in biometric applications remains relatively underexplored, and further studies involving larger and more diverse datasets are required to comprehensively assess its potential for reliable human recognition.

6. Conclusions

Smart devices play an increasingly vital role in enhancing the quality of life across various domains. However, their pervasive use involves the continuous collection of personal and sensitive user data; therefore, continuous authentication and reliable human recognition systems are essential for protecting user identity and privacy.

This study proposes a multimodal human recognition approach based on physiological signals, namely electrocardiography (ECG), photoplethysmography (PPG), and galvanic skin response (GSR), to enhance recognition performance. Statistical features are extracted from these signals and used as inputs to machine learning classifiers for biometric identification. The proposed approach was evaluated using two publicly available datasets: the CLAS dataset, comprising 60 healthy participants, and the MAUS dataset, consisting of 22 subjects. Experimental results demonstrate that the fusion of ECG, PPG, and GSR signals significantly improves classification performance, achieving mean recognition accuracies of 97% and 99% on the CLAS and MAUS datasets, respectively, using the K-Nearest Neighbors (KNN) classifier.

7. Future Work

Future research should focus on expanding and improving the generalizability of the datasets by increasing the number of participants and collecting physiological signals under diverse acquisition conditions and real-world scenarios. Such efforts would enable a more comprehensive assessment of the proposed approach and its robustness across varying environments.

In addition, integrating other biometric modalities, such as facial, fingerprint, and voice biometrics, with the proposed physiological signal-based framework may further enhance recognition performance and system reliability. Future studies should also investigate the impact of hyperparameter optimization on classifier performance. In the present work, all classifiers were implemented using their default parameter settings to ensure a fair and unbiased comparison. However, systematic hyperparameter tuning may lead to further improvements in recognition accuracy and overall model performance.

Furthermore, evaluating deep learning-based approaches represents a promising research direction. Although deep learning models typically require large amounts of training data, this limitation may be addressed through advanced data augmentation and synthetic data generation techniques. Methods such as Generative Adversarial Networks (GANs),

Variational Autoencoders (VAEs), diffusion models, and TimeGAN can be employed to generate realistic physiological signals and increase dataset diversity.

Finally, the deployment of the proposed framework within Internet of Things (IoT) environments warrants further investigation. Assessing its computational efficiency, real-time performance, and scalability in resource-constrained wearable and IoT devices is essential for enabling practical continuous authentication and biometric recognition applications.

Author Contributions: Author S.H. conceived the study and wrote the manuscript. Author H.S.K. performed the experiments and analyzed the data. Author O.G.E. supervised the project reviewed and approved the manuscript. All authors have read and agreed to the published version of the manuscript.

Funding: This research received no external funding.

Data Availability Statement: The original data presented in the study are openly available at https://dx.doi.org/10.21227/ybsw-yr53 and https://arxiv.org/abs/2111.02561 (accessed on 17 June 2026).

Conflicts of Interest: The authors declare that they have no competing interests.

References

1. Di Tecco, A.; Pistolesi, F.; Lazzerini, B. Elicitation of Anxiety without Time Pressure and its Detection using Physiological Signals and Artificial Intelligence: A Proof of Concept. *IEEE Access* **2024**, *12*, 22376–22393. [CrossRef]
2. Khan, P.; Ranjan, P.; Kumar, S. AT2GRU: A Human Emotion Recognition Model with Mitigated Device Heterogeneity. *IEEE Trans. Affect. Comput.* **2021**, *14*, 1520–1532. [CrossRef]
3. Shu, Y.; Yang, P.; Liu, N.; Zhang, S.; Zhao, G.; Liu, Y.-J. Emotion Distribution Learning Based on Peripheral Physiological Signals. *IEEE Trans. Affect. Comput.* **2022**, *14*, 2470–2483. [CrossRef]
4. Zhang, Y.; Zhao, G.; Shu, Y.; Ge, Y.; Zhang, D.; Liu, Y.J.; Sun, X. CPED: A Chinese Positive Emotion Database for Emotion Elicitation and Analysis. *IEEE Trans. Affect. Comput.* **2021**, *14*, 1417–1430. [CrossRef]
5. Albahdal, D.; Aljebreen, W.; Ibrahim, D.M. PainMeter: Automatic Assessment of Pain Intensity Levels from Multiple Physiological Signals Using Machine Learning. *IEEE Access* **2024**, *12*, 48349–48365. [CrossRef]
6. Piciucco, E.; Di Lascio, E.; Maiorana, E.; Santini, S.; Campisi, P. Biometric recognition using wearable devices in real-life settings. *Pattern Recognit. Lett.* **2021**, *146*, 260–266. [CrossRef]
7. Bianco, S.; Napoletano, P. Biometric Recognition Using Multimodal Physiological Signals. *IEEE Access* **2019**, *7*, 83581–83588. [CrossRef]
8. Blasco, J.; Peris-Lopez, P. On the Feasibility of Low-Cost Wearable Sensors for Multi-Modal Biometric Verification. *Sensors* **2018**, *18*, 2782. [CrossRef] [PubMed]
9. Albert, B.; Tullis, T. *Measuring the User Experience*; Google Books; Elsevier: Amsterdam, The Netherlands, 2022. Available online: https://books.google.com.eg/books?hl=en&lr=&id=L5xBEAAAQBAJ&oi=fnd&pg=PP1&dq=Albert (accessed on 2 November 2024).
10. Cho, M.K.; Kim, T.S. Canine Biometric Identification Using ECG Signals and CNN-LSTM Neural Networks. *IEEE Access* **2023**, *11*, 145732–145746. [CrossRef]
11. Ghorbani, R.; Reinders, M.J.T.; Tax, D.M. Personalized anomaly detection in PPG data using representation learning and biometric identification. *Biomed. Signal Process. Control* **2024**, *94*, 106216. [CrossRef]
12. Labati, R.D.; Piuri, V.; Rundo, F.; Scotti, F. MultiCardioNet: Interoperability between ECG and PPG biometrics. *Pattern Recognit. Lett.* **2023**, *175*, 1–7. [CrossRef]
13. Jeon, Y.; Kang, S.J. Multi-slice Nested Recurrence Plot (MsNRP): A robust approach for person identification using daily ECG or PPG signals. *Eng. Appl. Artif. Intell.* **2023**, *126*, 106799. [CrossRef]
14. Wan, L.; Liu, K.; Mengash, H.A.; Alruwais, N.; Duhayyim, M.A.; Venkatachalam, K. Deep learning-based photoplethysmography biometric authentication for continuous user verification. *Appl. Soft Comput.* **2024**, *156*, 111461. [CrossRef]
15. Yi, P.; Si, Y.; Fan, W.; Zhang, Y. ECG Biometrics Based on Attention Enhanced Domain Adaptive Feature Fusion Network. *IEEE Access* **2024**, *12*, 1291–1307. [CrossRef]
16. Albadawi, Y.; Shanableh, T. Hand-Crafted Features with a Simple Deep Learning Architecture for Sensor-Based Human Activity Recognition. *IEEE Sens. J.* **2024**, *24*, 28300–28313. [CrossRef]

17. Fauzan, M.R.A.; Rizal, A.; Hadiyoso, S. ECG Biometric using Statistical Feature of EEMD and VMD. In *Proceedings of the 2022 IEEE International Conference on Industry 4.0, Artificial Intelligence, and Communications Technology (IAICT), Bali, Indonesia, 28–30 July 2022*; IEEE: New York, NY, USA, 2022; pp. 113–118. [CrossRef]
18. Dempster, J. *The Laboratory Computer*; ScienceDirect: London, UK, 2001. Available online: https://www.sciencedirect.com/book/9780122095511/the-laboratory-computer (accessed on 2 November 2024).
19. Pham, T.; Lau, Z.J.; Chen, S.H.A.; Makowski, D. Heart Rate Variability in Psychology: A Review of HRV Indices and an Analysis Tutorial. *Sensors* **2021**, *21*, 3998. [CrossRef] [PubMed]
20. Ciccone, A.B.; Siedlik, J.A.; Wecht, J.M.; Deckert, J.A.; Nguyen, N.D.; Weir, J.P. Reminder: RMSSD and SD1 are identical heart rate variability metrics. *Muscle Nerve* **2017**, *56*, 674–678. [CrossRef] [PubMed]
21. Uwaechia, A.N.; Ramli, D.A. A Comprehensive Survey on ECG Signals as New Biometric Modality for Human Authentication: Recent Advances and Future Challenges. *IEEE Access* **2021**, *9*, 97760–97802. [CrossRef]
22. Padmakala, S. Modeling Authentication Accuracy in Medical Biometrics: A Machine Learning Approach with Performance Benchmarking. In *Proceedings of the 2025 3rd International Conference on Sustainable Computing and Smart Systems (ICSCSS), Coimbatore, India, 20–22 August 2025*; IEEE: New York, NY, USA, 2025; pp. 1888–1895. [CrossRef]
23. Zhang, Z.; Lu, H.; Zhao, Q.; Wen, K.; Liu, B. PPG Sensor-Based Biometric Identification and Physiological Analysis via Temporal-Frequency Disentanglement with Liquid Neural Networks. *IEEE Sens. Lett.* **2025**, *9*, 6008804. [CrossRef]
24. Zheng, X.X.; Taha, B.; Rahman, M.M.U.; Masood, M.; Hatzinakos, D.; Al-Naffouri, T. Multimodal biometric authentication using camera-based PPG and fingerprint fusion. *Pattern Recognit. Lett.* **2025**, *197*, 1–7. [CrossRef]
25. Rumelhart, D.E.; Hinton, G.E.; Williams, R.J. Learning representations by back-propagating errors. *Nature* **1986**, *323*, 533–536. [CrossRef]
26. Cox, D.R. The Regression Analysis of Binary Sequences. *J. R. Stat. Soc. Ser. B Methodol.* **1958**, *20*, 215–232. [CrossRef]
27. Cortes, C.; Vapnik, V. Support-vector networks. *Mach. Learn.* **1995**, *20*, 273–297. [CrossRef]
28. Breiman, L. Random Forests. *Mach. Learn.* **2001**, *45*, 5–32. [CrossRef]
29. Cover, T.; Hart, P. Nearest neighbor pattern classification. *IEEE Trans. Inf. Theory* **1967**, *13*, 21–27. [CrossRef]
30. Quinlan, J.R. Induction of decision trees. *Mach. Learn.* **1986**, *1*, 81–106. [CrossRef]
31. Markova, V. Database for Cognitive Load Affect and Stress recognition. In *IEEE Dataport*; IEEE: New York, NY, USA, 2020. [CrossRef]
32. Beh, W.-K.; Wu, Y.-H.; An-Yeu. MAUS: A Dataset for Mental Workload Assessmenton N-back Task Using Wearable Sensor. *arXiv* **2021**, arXiv:2111.02561. [CrossRef]
33. Xu, Y.; Wang, Z.; Liu, X. Photoplethysmogram (PPG)-Based Biometric Identification Using 2D Signal Transformation and Multi-Scale Feature Fusion. *Sensors* **2025**, *25*, 4849. [CrossRef] [PubMed]
34. Lee, J.-N.; Kwak, K.-C. ECG-Based Biometrics Using a Deep Network Based on Independent Component Analysis. *IEEE Access* **2022**, *10*, 12913–12926. [CrossRef]
35. Aly, H.A.; Di Pietro, R. PulseOblivion: An Effective Session-Based Continuous Authentication Scheme Using PPG Signals. *IEEE Access* **2023**, *11*, 124213–124227. [CrossRef]
36. Hinatsu, S.; Suzuki, D.; Ishizuka, H.; Ikeda, S.; Oshiro, O. Evaluation of PPG Feature Values Toward Biometric Authentication Against Presentation Attacks. *IEEE Access* **2022**, *10*, 41352–41361. [CrossRef]
37. Hinatsu, S.; Matsuda, N.; Ishizuka, H.; Ikeda, S.; Oshiro, O. Identification of PPG Measurement Sites Toward Countermeasures Against Biometric Presentation Attacks. *IEEE Access* **2022**, *10*, 118736–118746. [CrossRef]
38. Garg, R.; Pathak, P.; Singh, M.P. A multimodal biometric recognition system based on Fingerprints, Iris and ECG via Swin Transformer and CNN Model. *Syst. Soft Comput.* **2025**, *7*, 200369. [CrossRef]
39. Mancilla-Palestina, D.E.; Jimenez-Duarte, J.A.; Ramirez-Cortes, J.M.; Hernandez, A.; Gomez-Gil, P.; Rangel-Magdaleno, J. Embedded System for Bimodal Biometrics with Fiducial Feature Extraction on ECG and PPG Signals. In *Proceedings of the 2020 IEEE International Instrumentation and Measurement Technology Conference (I2MTC), Dubrovnik, Croatia, 25–28 May 2020*; IEEE: New York, NY, USA, 2020; pp. 1–6. [CrossRef]
40. Dhyanesh, S.J.; Sarathy, S.P.; Kesavan, H.; Vallisree, S. ML Based Enhanced Authentication Using ECG and PPG Signals for Remote Monitoring of Patients. *Prim. Sci. Eng.* **2024**, *4*, 26–30. [CrossRef]
41. Ashwini, K.; Murthy, K.; Raviraja, S.; Srinidhi, G.A. A Novel Multimodal Biometric Person Authentication System Based on ECG and Iris Data. *BioMed Res. Int.* **2024**, *2024*, 8112209. [CrossRef] [PubMed]
42. Roy, A.; Satija, U. A Novel Deep Metric Learning-Based State-Stable and Noise-Aware Biometric Authentication Framework Using Seismocardiogram Signals. *IEEE Trans. Biom. Behav. Identity Sci.* **2025**, *7*, 246–255. [CrossRef]
43. Kumari, S.; Jyotishi, D.; Das, S.; Dandapat, S. Analyzing the Effect of Segmentation on PCG Based Biometric System. In *Proceedings of the 2022 IEEE 19th India Council International Conference (INDICON), Kochi, India, 24–26 November 2022*; IEEE: New York, NY, USA, 2022; pp. 1–6. [CrossRef]

44. Mehmood, A.; Hannan, A.; Khan, M.U.; Naqvi, S.Z.H.; Faraz, M.; Aziz, S. Biofusion: Expanding Biometric Horizons with ECG and PCG Integration. In *Proceedings of the 2023 3rd International Conference on Digital Futures and Transformative Technologies (ICoDT2), Islamabad, Pakistan, 3–4 October 2023*; IEEE: New York, NY, USA, 2023; pp. 1–6. [CrossRef]
45. Salturk, T.; Kahraman, N. The Role of Multiple Data Characteristics in EEG-Based Biometric Recognition: The Impact of States, Channels, and Frequencies. *IEEE Access* **2025**, *13*, 29994–30009. [CrossRef]

Disclaimer/Publisher's Note: The statements, opinions and data contained in all publications are solely those of the individual author(s) and contributor(s) and not of MDPI and/or the editor(s). MDPI and/or the editor(s) disclaim responsibility for any injury to people or property resulting from any ideas, methods, instructions or products referred to in the content.